

## VIBRATION CONTROL FOR STEEL TUBULAR TOWERS OF HORIZONTAL AXIS WIND TURBINES

**Matheus Alves Pereira**

*matheus\_alves1996@hotmail.com*

*Departamento de Engenharia Civil, Universidade Federal de Pernambuco*

*Av. Acadêmico Hélio Ramos, s/n, 50740-530, Recife-PE, Brazil*

**Douglas Mateus de Lima**

*douglasortoedro@gmail.com*

*Núcleo de Tecnologia, Universidade Federal de Pernambuco*

*Av. Campina Grande, s/n, 55014-900, Caruaru-PE, Brazil*

**Pablo Aníbal López-Yáñez**

*lopez.yanez@yahoo.com.br*

*Departamento de Engenharia Civil, Universidade Federal de Pernambuco*

*Av. Acadêmico Hélio Ramos, s/n, 50740-530, Recife-PE, Brazil*

**Abstract.** This paper analyzes the effectiveness of three types of vibration control, namely, Tuned Mass Damper (TMD), Active Mass Damper (AMD) and a Hybrid Mass Damper (HMD), applied to a steel tubular tower, 120 m high, for an onshore Horizontal Axis Wind Turbine (HAWT). For this, the tower was modeled using beam (own code) and shell and solid finite elements (via ANSYS). In all cases, the insertion of the control device was idealized at the top of the tower. The theory proposed by Den Hartog was used to determine the coefficients of the absorber and the Linear Quadratic Regulator (LQR) was applied to obtain the optimal control variables introduced by the hydraulic actuators. It was observed a reduction of the root mean square (r.m.s) of displacements of the top of the tower with control in relation to the without control displacements, when subjected to a harmonic and resonant action to the first mode of vibration of the uncontrolled structure: 67.78% for the TMD and 71.64% for the AMD in a transient excitation; 93.87% for the TMD and 95.26% for the AMD in a permanent excitation. In addition, the effective displacements (r.m.s) with the use of HMD were smaller compared to the TMD results, presenting a reduction of 26.68% in the transient excitation and 39.46% in the permanent excitation.

**Keywords:** Wind turbine tower, Dynamic analysis, Vibration control.

## 1 Introduction

In the 21st century, the global water crisis and environmental issues resulted in an accelerated growth in the deployment of increasingly large onshore and offshore wind turbines, with increasingly high towers, in search of technically feasible and economically viable winds. Therefore, the technical development, trade and installation of wind turbines in the world has advanced fastly, so that the generation of energy from thermoelectric, nuclear and hydroelectric power plants has been complemented and/or replaced by the production of such equipment (Hau, 2006 [1]).

The global growth of installed wind capacity in recent years has established an annual record of 63,633 MW in 2015; resulting in a cumulative installed wind capacity of 591 GW at the end of 2017 (GWEC, 2019 [2]). In Brazil, wind power production reached 14.34 GW of installed capacity in 568 wind farms and more than 7,000 wind turbines in 12 states, with the states of the Northeast Region, where the records of attendance exceed 70% of the energy produced in this region, which account for most of Brazilian production (September data according to Abeeólica, 2018 [3]). This shows that the cost of wind energy is the most competitive and viable amongst the renewable energy sources compared to the conventional ones (Burton et al., 2011 [4] and Manwell et al., 2009 [5]).

For this reason, Brazilian political, social and technical issues have been studied in order to make feasible and further develop the use of this type of energy to produce electricity (Juárez et al., 2014 [6]). Specifically, the state of Pernambuco has carried out, over the last years, a series of actions, with the objective of fomenting the renewable energy sector (Atlas..., 2017 [7]). Among these, we highlight the attraction of industries to the Suape Wind Pole, that resulted in the installation of a group of companies to manufacture wind turbines, tubular towers, large blades and steel forged. For example, the wind power plants of Santa Brigida located in Caetés, Pedra and Paratama cities of Agreste region of Pernambuco and the wind power plants of Santo Estevão in Araripina city of Chapada region of Araripe totalizing more than 600 towers of 80 m high for support wind turbines in operation in the state, evidencing the growth of this type of energy.

In view of the vast potential of wind power that can be used in the state of Pernambuco, the size of the wind turbines to be used in the future tends to be increasing and more powerful, making it necessary to install these equipments under the action of more intense and continuous winds and thus causing the dimensions of the towers of these wind turbines to be continuously increased. Particularly, the height of the tower is an essential parameter for capturing stable high-altitude winds; however, the cost of this, which can exceed 20% of the wind turbine overall cost (Hau, 2006 [1] and Yoshida, 2006 [8]), makes the height increase a disadvantage. In addition, the transport and the assembly of the tower become more expensive. Therefore, the design and installation of larger wind turbines makes it necessary to have higher and higher towers that require more elaborate structural analysis, stability and dynamics, resulting in a more complex design.

Thus, increasing the towers height, the vibration effects on the wind turbine components are greatly increased, so that in the last decades researchers and manufacturers of wind turbine components have sought solutions to mitigate the vibrations from the operation of mechanical components and wind and seismic actions (Menezes et al., 2018 [9]). Even in situations where these structures can withstand such dynamic actions, without necessarily suffering structural damage, the fatigue effects of the constituent materials should not be overlooked.

To achieve the balance between safety and economic efficiency in large wind turbine design, the structural control to mitigate excessive structure responses is a viable option. In this way, passive, active, hybrid and semi-active control systems are valuable alternatives for the control of vibrations of large wind turbine towers. Even considering the studies already carried out and the numerous practical applications of structural control in bridges, in telecommunications towers and in tall buildings, the research and application of control systems for wind turbine towers are relatively recent topics.

Hence, this paper proposes to analyze the dynamic behavior of a vibration control device for a 120 m high steel tubular tower of a 3.2 MW Horizontal Axis Wind Turbine (HAWT), through an active, passive and hybrid control system.

## 2 Vibration control theory

### 2.1 Passive control vibration

For the vibration control methodology used in this paper, the theoretical development of the TMD proposed by Den Hartog (1947) [10] was initially used for systems with two degrees of freedom, one of which is necessary to describe the movement of the main mass (the structure to be controlled) and the second one referring to the secondary mass (mass of the vibration absorber). The TMD is a device consisting of a mass, a spring (or a combination of springs) and a damper (or a damper assembly) that are attached to the main structure in order to reduce/control its dynamic response. The frequency of the absorber is tuned in a certain frequency of the main structure. When this frequency is excited, the absorber vibrates out of phase in relation to the movement of the structure, dissipating the energy contained in the main structure by the movement of the absorber.

The absorber parameters (mass  $m_t$ , stiffness  $k_t$ , and damping  $c_t$ ) will be determined according to their design requirements (frequency tuning of the absorber). The main structure is represented by its modal parameters (mass  $m_p$ , stiffness  $k_p$ , and damping  $c_p$ ) referring to the mode of vibration that will be controlled. It should be noted that the TMD theory was applied to a non-damped main structure, considering the low structural damping of the tower studied here (damping ratio of 0.8%, as indicated by Brazilian Standard ABNT, 1988 [11] and Blevins, 2001 [12]).

Writing the motion equations of the system and applying the complex numbers for resolution when the main structure is subjected to a harmonic excitation, we obtain:

$$a_p = a_{est} \left[ \frac{(\beta^2 - f^2)^2 + (2\zeta\beta)^2}{(2\zeta\beta)^2(\beta^2 - 1 + \mu\beta^2)^2 + [\mu f^2\beta^2 - (\beta^2 - 1)(\beta^2 - f^2)]^2} \right]^{\frac{1}{2}} \quad (1)$$

which is the steady-state amplitude of the mass  $m_p$ , and

$$a_t = a_{est} \left[ \frac{f^4 + (2\zeta\beta)^2}{(2\zeta\beta)^2(\beta^2 - 1 + \mu\beta^2)^2 + [\mu f^2\beta^2 - (\beta^2 - 1)(\beta^2 - f^2)]^2} \right]^{\frac{1}{2}} \quad (2)$$

which is the steady-state amplitude of the mass  $m_t$  (Rao, 2011 [13]). Where:  $\mu$  is the mass ratio between the absorber and main mass:

$$\mu = \frac{m_t}{m_p} \quad (3)$$

$f$  is the ratio of square angular frequency of the absorber and main mass:

$$f = \frac{\omega_t}{\omega_p} \quad (4)$$

$\beta$  is the ratio between the angular frequencies of the excitation ( $\bar{\omega}$ ) and main mass:

$$\beta = \frac{\bar{\omega}}{\omega_p} \quad (5)$$

$a_{est}$  is the static deflection of the main system, Eq. (6), and  $\zeta$  is the damping ratio of the vibration absorber, according to Eq. (7).

$$a_{est} = \frac{F_0}{k_p} \quad (6)$$

which,  $F_0$  is the amplitude of the proposed harmonic excitation.

$$\zeta = \frac{c_t}{c_c} \quad (7)$$

where,  $c_c$  is the “critical” damping constant, given by:

$$c_c = 2 m_t \omega_p \quad (8)$$

With the addition of the absorber to the system, it is intended to reduce the amplitude peaks of the main mass to the lowest possible values. The amplitude peaks of the main structure are infinite when the damping of the absorber is zero (resonance) or infinite. However, there is an intermediate value of damping for which these peaks are minimal, since the work performed by the damping force is maximum.

According to Den Hartog (1947) [10], by evaluating the values  $\beta$  in Eq. (1), the amplitude of the main mass becomes independent of  $\zeta$  (in the two fixed points of the graph  $a_p$  versus  $\beta$ ) when:

$$f = \frac{1}{1 + \mu} \quad (9)$$

which is the tuning required as a function of the absorber mass.

Finally, the optimal damping values can be calculated by substituting Eq. (9) into Eq. (1), deriving the resulting expression from  $\beta$  and equating to zero to have horizontal tangents at fixed points. Therefore, after long algebraic work and taking a convenient average value of the optimal fixed points of damping, we obtain:

$$\zeta_{optimum}^{medium} = \left[ \frac{3 \mu}{8(1 + \mu)^3} \right]^{\frac{1}{2}} \quad (10)$$

Thus, by using the damping value above, there is an almost horizontal tangent at each of the fixed points. The stiffness value of the tuned absorber can be calculated using Eq. (3) and (4):

$$k_t = f^2 k_p \mu \quad (11)$$

The design values of the vibration absorber coefficients are calculated by considering that the tower movement is governed predominantly but independently by the first two natural modes of vibration (the first two flexural modes having practically equal vibration frequencies). Thus, the absorber is independently tuned to the two natural frequencies whose modes define movements according to the first two vibration modes of the tower. The optimal values of the absorber coefficients are then obtained as if these two modes of vibration of the tower were represented by two independent systems of one degree of freedom (dof) each, in order to make feasible the application of Den Hartog's theory.

The TMD is preferably allocated where the deflections of the structure are larger; in this case, the TMD motion is associated with an added translational dof near the tower top. Thus, the mass, stiffness, and damping matrices of the coupled system (tower-absorber) come from the addition of the aforementioned dof.

Therefore, by means of the modal mass, stiffness, and damping values, the coefficients corresponding to the modes of vibration of the main system to be controlled are obtained. Then, starting from the choice of mass ratio  $\mu$ , the stiffness and damping of the absorber are obtained in two directions transverse to the tower and perpendicular to each other (Fig. 1a). It is pointed out that if the

actuating excitation does not coincide with the direction of any of the axes where the stiffness and damping of the absorber are arranged, there will be the vectorial combination thereof for the stiffness and damping resulting from the passive controller in any direction of the cross-section of the tower.

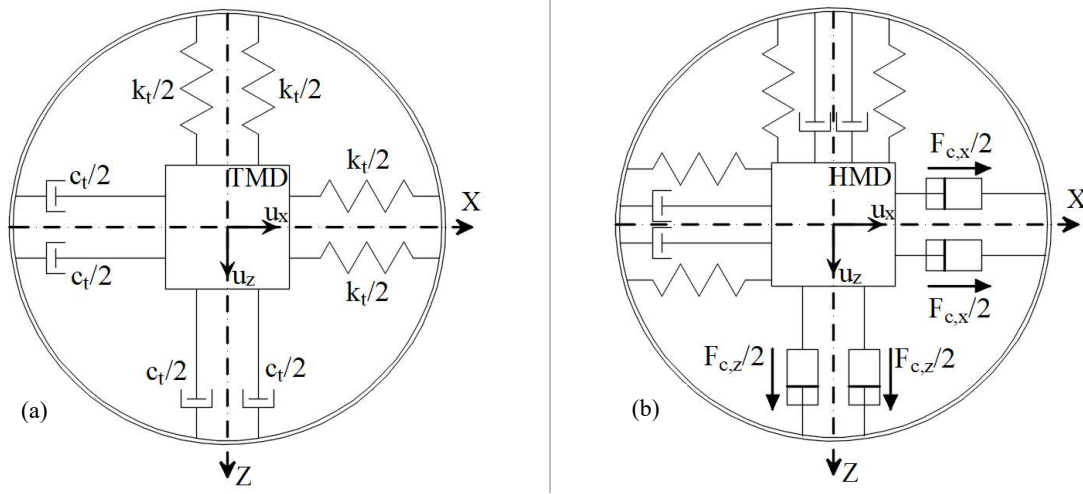


Figure 1. Schemes of passive (a) and hybrid (b) Dynamic Vibration Absorbers (DVA) with two degrees of freedom.

## 2.2 Hybrid vibration control

The translational hybrid vibration absorber of two degrees (Fig. 1b) is defined similarly to the dynamic passive vibration absorber with two degrees of freedom of translation. Hydraulic actuators were added to the system in order to convert the TMD into a Hybrid Mass Damper (HMD), which is applied to the tower top to obtain a hybrid control system.

This model is idealized as part of a full state feedback control system, that is, the actuators apply forces of magnitudes and directions pre-established by the controller. These forces are generated from the signals received from the sensors positioned in a way measure all model state variables. Thus, for a tower model with 8 beam finite elements that already shows good accuracy in relation to the structure of the excessively discrete tower, with respect to the most significant global vibration modes for dynamic final tower response, it is necessary to position the sensors every 15 m of tower length, for example.

Working in the field of analysis and design of modern control systems, it is convenient to represent the differential equations that generate the movement of a dynamic system in the states space (Moutinho, 2007 [14]). This analysis involves three types of variables in its modeling, namely: state variables, input variables and output variables. The state variables of a dynamic system are quantities whose set of values determines the state of the system (Junkins and Kim, 1993 [15]). Input variables are quantities related to external actions or control forces/moments applied to the structure. The output variables are related to the input or state variables that can be measured, since in many practical situations, not all states or inputs are available for measurement.

Considering the static condensation (Clough and Penzien, 2003 [16]; Chopra, 2012 [17] and Humar, 2002 [18]) of the dynamic system that represents the behavior of the tower, in order to dynamically study the horizontal translation dof, the dynamic motion equation of the structure-DVA takes the following form:

$$\left[ \widetilde{M}_u \right] \{ \ddot{\tilde{u}} \} + \left[ \widetilde{C}_u \right] \{ \dot{\tilde{u}} \} + \left[ \widetilde{K}_u \right] \{ \tilde{u} \} = \left[ \widetilde{J} \right] \{ \tilde{F}_u \} + \left[ \widetilde{J}_c \right] \{ \tilde{F}_c \} \quad (12)$$

where:  $\left[ \widetilde{M}_u \right]$ ,  $\left[ \widetilde{C}_u \right]$ , and  $\left[ \widetilde{K}_u \right]$  are, respectively, the mass, damping and stiffness matrices in relation to the horizontal translation dof of the tower-absorber assembly, dimension  $\left[ (n_c + r_c), (n_c + r_c) \right]$ ;  $\{ \tilde{u} \}$  is the translational displacements vector, order  $(n_c + r_c)$ ;  $\{ \tilde{F}_u \}$  is the vector of external forces, order

$m_c$ ;  $[\bar{J}]$  is the positioning matrix of external forces, dimension  $[(n_c + r_c), m_c]$ , which, in this case, is an identity matrix, because the forces act in all horizontal translation dof;  $\{\bar{F}_c\}$  is the vector of control forces, order  $r_c$ ;  $[\bar{J}_c]$  is the positioning matrix of control forces, dimension  $[(n_c + r_c), r_c]$ ;  $n_c$  represents the number of horizontal dof of the condensed system without absorber;  $m_c$  represents the number of horizontal external forces applied;  $r_c$  represents the number of horizontal control forces of the actuator according to the degree of freedom of the vibration absorber; and, consequently,  $(n_c + r_c)$  represents the number of horizontal translations dof of the tower-absorber assembly.

In the hybrid vibration absorber is considered that external forces are not applied, but only a control force imposed by the actuator. Thus, the vector  $\{\tilde{F}_u\}$  takes the following form:

$$\{\tilde{F}_u\} = \begin{Bmatrix} \tilde{F}_{u1} \\ \tilde{F}_{u2} \\ \vdots \\ \tilde{F}_{un_c} \\ 0 \end{Bmatrix} \quad (13)$$

the control force vector ( $r_c = 1$ ) is:

$$\{\bar{F}_c\} = \bar{F}_c \quad (14)$$

and the matrix  $[\bar{J}_c]$  is given by:

$$[\bar{J}_c] = \begin{bmatrix} [0]_{(n_c+r_c-2),1} \\ -1 \\ 1 \end{bmatrix} \quad (15)$$

in which, terms 1 and  $-1$  refer to the action and reaction, from the control force applied by the actuator to the absorber and the respective reaction in the tower where the actuator is attached, respectively.

Finally, for passing to the state space, we isolate the vector  $\{\ddot{u}\}$  from Eq. (12) and define the vector of state variables  $\{X\}$ , order  $2(n_c + r_c)$ , given by:

$$\{X\} = \begin{Bmatrix} \{\tilde{u}\} \\ \{\dot{\tilde{u}}\} \end{Bmatrix} \quad (16)$$

obtaining the STATE EQUATION of the system:

$$\{\dot{X}\} = [A]\{X\} + [B]\{\tilde{F}_u\} + [B_c]\{\bar{F}_c\} \quad (17)$$

which will be solved by applying a linear transformation diagonalizing the state matrix  $[A]$ :

$$[A] = \begin{bmatrix} [0] & [I] \\ -[\tilde{M}_u]^{-1}[\tilde{K}_u] & -[\tilde{M}_u]^{-1}[\tilde{C}_u] \end{bmatrix} \quad (18)$$

$[B]$  is the input matrix of the external forces applied to the horizontal translation dof:

$$[B] = \begin{bmatrix} [0] \\ [\widetilde{M}_u]^{-1} [\bar{J}] \end{bmatrix} \quad (19)$$

and,  $[B_c]$  is the input matrix of the control forces applied to the vibration absorber:

$$[B_c] = \begin{bmatrix} [0] \\ [\widetilde{M}_u]^{-1} [\bar{J}_c] \end{bmatrix} \quad (20)$$

Finally, we have the output equation that defines the output vector  $\{YY\}$  of the system as a linear combination of the state variables and the control input variables:

$$\{YY\} = [CC]\{X\} + [DD]\{\bar{F}_c\} \quad (21)$$

where:  $[CC]$  is the output matrix that determines the relationship between the state system and the output system;  $[DD]$  is the feed-forward matrix; and,  $p_c$  represents the number of output variables.

### 2.3 Active vibration control

An Active Mass Damper (AMD) was implemented to evaluate the behavior of the system controlled by a purely active absorber and to have information of the energy expenditure necessary to perform the control of the tower by this type of absorber. The AMD of two degrees of freedom consists of a system composed of a mass guided exclusively by hydraulic actuators, without springs and dampers. Thus, from the HMD, the stiffness and damping matrices are obtained by assigning null values to the parameters of stiffness and damping of the absorber (that is,  $k_t = 0$  and  $c_t = 0$ ). The mass matrix remains unchanged from the hybrid system, depending only on the mass ratio  $\mu$ . In addition, the external and control forces vectors have the same format as those in Eq. (14) and (15), respectively.

### 2.4 Linear optimal control

In active and hybrid control systems is necessary to determine the values of the input variables that will be applied by the actuators. In this way, the design of stable control systems based on quadratic performance indexes (or cost function) will be considered in this item. We intend to choose the control vector  $\{\bar{F}_c\}$  such that a given performance index is minimized. Thus, a quadratic performance index  $J$ , where the limits of integration are 0 and  $\infty$ , is given by:

$$J = \int_0^{\infty} L(\{X\}, \{\bar{F}_c\}) dt \quad (22)$$

where  $L(\{X\}, \{\bar{F}_c\})$  is a quadratic function that leads to linear control laws (Meirovitch, 1990 [19]):

$$\{\bar{F}_c\} = -[KG]\{X\} \quad (23)$$

where  $[KG]$  is the optimal feedback gain matrix, dimension  $[r_c, 2(n_c + r_c)]$ , of the optimal control vector. The design of optimum control systems, based on quadratic performance indexes, is reduced to the determination of matrix elements. The performance index for the control system is:

$$J = \int_0^{\infty} (\{X\}^T [Q] \{X\} + \{\bar{F}_c\}^T [R] \{\bar{F}_c\}) dt \quad (24)$$

where:  $[Q]$  is the state ponderation matrix, which is positive-(semi)definite real symmetric for systems with real matrices and vectors, dimension  $[2(n_c + r_c), 2(n_c + r_c)]$ ;  $[R]$  is the control ponderation matrix, which is positive-definite real symmetric for systems with real matrices and vectors, dimension  $[r_c, r_c]$ . The control forces vector  $\{\bar{F}_c\}$  is unconstrained, except those of a practical interest.

The second term on the right-hand side of Eq. (24) accounts for the energy expenditure of the control signals, which will be a determining factor for the operation of the control system, because the intensity of the control force will be limited by the capacity of the hydraulic actuators.

To solve the optimization problem, we substitute Eq. (23) into (17):

$$\{\dot{X}\} = ([A] - [B_c][KG])\{X\} + [B]\{\tilde{F}_u\} \quad (25)$$

in which, we assume that the matrix  $([A] - [B_c][KG])$  is stable, or that its eigenvalues have negative real parts. Substituting Eq. (23) into (24):

$$J = \int_0^{\infty} \{X\}^T \left( [Q] + [KG]^T [R][KG] \right) \{X\} dt \quad (26)$$

According to Ogata (1997) [20], we use the Lyapunov approach to solve this optimization problem:

$$\{X\}^T \left( [Q] + [KG]^T [R][KG] \right) \{X\} = -\frac{d}{dt} \left( \{X\}^T [P] \{X\} \right) \quad (27)$$

where  $[P]$  is positive-definite real symmetric matrix (real parameters). Developing the equation above:

$$\{X\}^T \left( [Q] + [KG]^T [R][KG] \right) \{X\} = -\{\dot{X}\}^T [P] \{X\} - \{X\}^T [P] \{\dot{X}\} \quad (28)$$

replacing Eq. (26) without the vector of external forces that may be associated with external disturbances acting on the system, and observing that this equation must be true for any  $\{X\}$ , we obtain:

$$([A] - [B_c][KG])^T [P] + [P]([A] - [B_c][KG]) = -\left( [Q] + [KG]^T [R][KG] \right) \quad (29)$$

By Lyapunov's second method (Lyapunov, 1992 [21]), if  $([A] - [B_c][KG])$  is a stable matrix, thus there is a  $[P]$  positive-definite matrix that satisfies Eq. (29). Therefore, the procedure to be followed is to determine the  $[P]$  elements of and verify whether it is positive definite.

In order to obtain the solution to the quadratic optimal control problem, we write the matrix  $[R]$  as:

$$[R] = [T]^T [T] \quad (30)$$

where  $[T]$  is a nonsingular matrix. Then, Eq. (29) can be rewritten and then minimized the quadratic form below that is required in the case of minimization of  $J$  with respect to  $[KG]$ :

$$\{X\}^T \left[ [T][KG] - \left( [T]^T \right)^{-1} [B_c]^T [P] \right]^T \left[ [T][KG] - \left( [T]^T \right)^{-1} [B_c]^T [P] \right] \{X\} \quad (31)$$

a function of  $[KG]$ . Since this last expression is nonnegative, the minimum occurs when it is zero. Thus:

$$[KG] = [R]^{-1} [B_c]^T [P] \quad (32)$$

which is the optimal gain matrix required. Finally, the  $[P]$  matrix from the above expression must satisfy the following expression based on Eq. (29):

$$[A]^T [P] + [P][A] - [P][B_c][R]^{-1}[B_c]^T [P] + [Q] = [0] \tag{33}$$

that is called the matrix Ricatti equation. Its resolution is obtained by the process of diagonalization, as presented in Kwakernaak and Sivan (1972) [22].

### 3 Tower modeling

A S355J2 steel tubular tower (design by Lima et al., 2018 [23]; Fig. 2) supporting an SWT-3.2-113 (Siemens, 2014 [24]) wind turbine was considered, according to the characteristics specified in Table 1.

The modeling of the tower was done using the Finite Element Method – MEF (Cook et al., 2002 [25]), considering non-linear geometric elastic behavior. Initially, a code was implemented in Mathcad v.15 (2012) [26], in which the tower was modeled as a structure clamped at the base and free at the top (cantilevered), using 8 dof beam finite elements (4 dof per node: axial and transverse translations, flexional and torsional rotations). An analysis was made of the required level of discretization (convergence analysis). It was noticed that a discretization with about 16 beam elements is already sufficiently accurate to the modal analysis necessary for the design of the control device proposed.

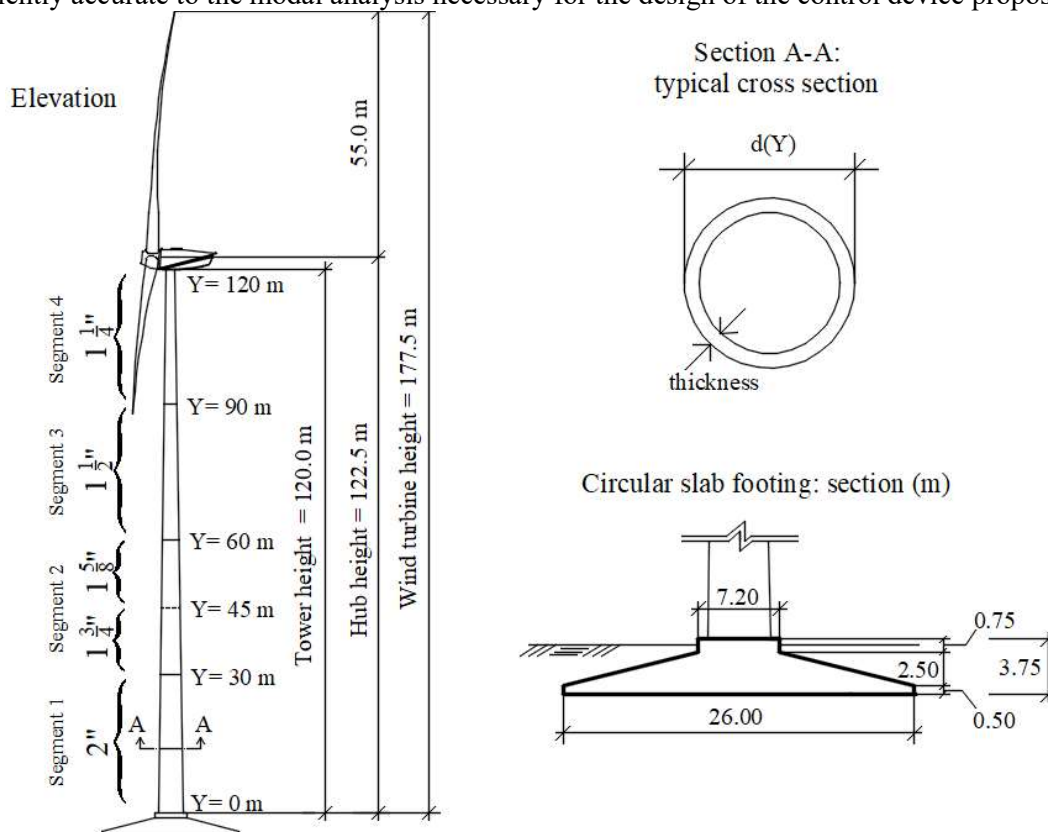


Figure 2. Tower-foundation design, off-scale (Lima et al., 2018 [23]).

Moreover, a finite element model was created in the software ANSYS r.14.5 (2012) [27], in which the tower was also clamped in the base (Fig. 3a) and discretized by 7272 shell elements with 4 node and 6 dof per node (Fig. 3b). The nacelle was modeled with tetrahedral solid finite elements, designated by SOLID187 (Fig 3c), with 10 nodes and 3 translational dof per node; representing it by a uniform mass. The main reason that led to the use of two finite element models was the need to evaluate the reliability and accuracy of the numerical results obtained.

Table 1. Parameters of the wind turbine manufacturer (Siemens, 2014 [24]).

Parameters	
IEC (International Electrotechnical Commission) Class	IIA
Rated power (MW)	3.2
Rotor diameter (m)	113.0
Blade length (m)	55.0
Swept area (m <sup>2</sup> )	10,000
Hub height (m)	79.5 – 142.0 (used 122.5 m)
Power regulation	Pitch regulated
Annual output at 8.5 m/s	14,402 MWh
Nacelle weight (ton)	78
Rotor weight (ton)	67

The results of the modal analysis performed by Lima (2018) [28] for both the shell and beam finite element model are similar for the global vibration modes, mainly with respect to the 1st mode of vibration of the tower that is more susceptible to excitation. Therefore, the beam FE model can be used as a representative of the dynamic behavior of the tower when it is subjected to the harmonic excitations resonant to its fundamental frequency.

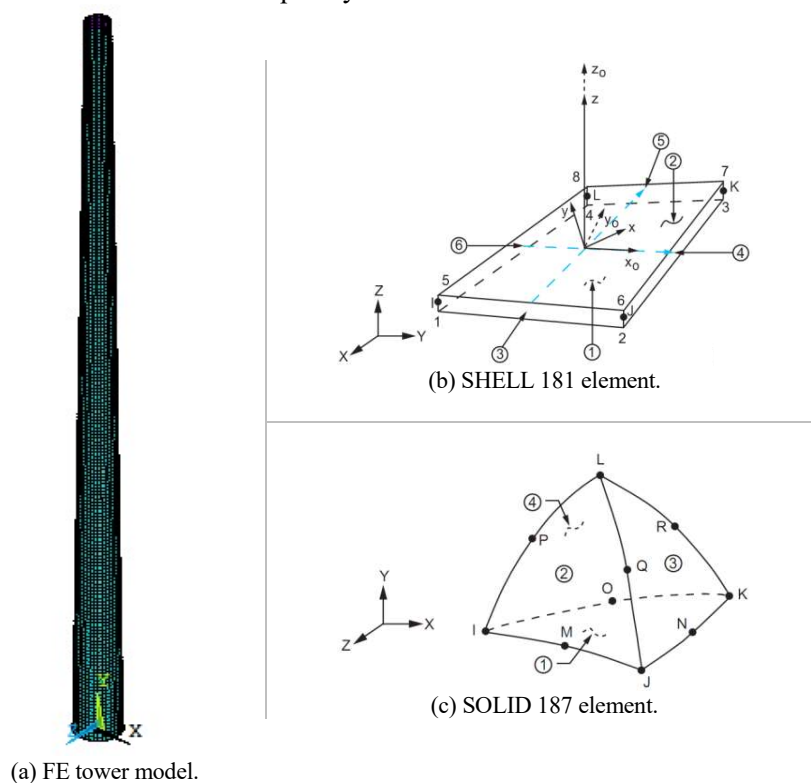


Figure 3. Model and finite elements used.

For excitation modeling, the terms amplitudes of the vector of forces applied horizontally to the tower were calculated using the parameters established by ABNT (1988) [11]: fluctuating component of the wind was established according to the difference between the peak velocity pressure and the main velocity pressure; and a horizontal force from the nacelle-rotor system applied to the top of the tower (according to Asibor et al., 2015 [29]).

The fluctuating component of the wind and the horizontal force transmitted by the rotor to the top were adopted according to a harmonic excitation considered resonant to the fundamental mode of vibration of the tower. In this way, it was considered that the tower vibrates around the equilibrium position determined by the action coming from the main wind speed (Franco, 1993 [30]). The amplitude of the force applied to the tower top has an order of magnitude 100 times greater than the

other amplitudes that corroborates with the excitation of its fundamental mode. It is also commented that the random effect of the wind action in the determination of the force vector was not considered, but only the intensity of the wind action that corresponds to its fluctuating component (wind gusts).

## 4 Analysis and Results

### 4.1 Passive vibration control of tower

In order to design a dynamic vibration absorber with two degrees of freedom that is able to control the oscillations according to the lateral directions X and Z, it is assumed that the movement according to the direction X of the tower is governed by the first mode of vibration (1st flexional mode in the XY-plane) and that the movement according to the Z direction is governed by the second mode (1st flexional mode in the YZ-plane). This fact is possible because it is a symmetrical structure, resulting in the first non-coupled modes of vibration (flexional XY and YZ). Thus, the absorber is designed to directly control the first two flexural modes of vibration of the tower, but having its utility directed to the control of the tower as a whole, since the vectorial composition of the stiffness and damping of the absorber allows the control in any direction transverse to the tower. Moreover, exclusively for the purposes of designing the absorber, the modal dampings associated with the 1st vibration modes of the tower are neglected in order to allow the application of Den Hartog's theory.

The modal mass and stiffness from the 1st tower vibration modes are given in Table 2. For the design of the absorber, the mass of the DVA is equal to 3% of the total mass of the tower (that is equal to 8.534 E5 kg), differently than some authors suggest that it is 0.5 to 1.0% (Housner et al., 1997 [31]). The tower is a large structure, so a greater mass percentage is needed to attenuate its vibrations without there being an amplitude of displacement exacerbated of the DVA, because there is a space limitation at the top of the tower (the top diameter of the analyzed model is 3.5 m). Thus, the DVA mass was adjusted in order to maintain its vibration amplitude limited to the space within the tubular structure of the tower.

With the values of the modal mass of the tower and the mass of the absorber, the parameters  $\mu$  (18.651%) and  $f$  (0.843), respectively, are determined using Eq. (3) and (4). Applying these values and the modal stiffness to Eq. (11), the stiffness required for the absorber is obtained. Finally, the damping constant is calculated by Eq. (7), (8), and (10). Table 2 shows the values of the vibration absorber parameters valid for both the X and Z directions.

Table 2. Modal parameters for the DVA design.

Structure type	Mass (kg)	Stiffness (N/m)	Damping (kg/s)
Tower	1.37263 E5	4.79351 E5	-
DVA	2.56014 E4	6.35067 E4	1.95797 E4

The absorber mass of 25601.4 kg is composed of a steel box (1.00 x 1.00 x 2.25 m) filled with lead. Lead was used as fill material because of its high specific mass (11340 kg/m<sup>3</sup>) and, consequently, reduction of the volume of the control device. Thus, given the parameters of the vibration absorber, the stiffness, mass, and damping matrices of the vibration-coupled tower-absorber system are assembled.

From the spectral matrix  $[\Lambda]$  of the state matrix  $[A]$ , we obtain the angular frequencies of the tower-absorber system, via the representation of poles in the complex plane (root locus method). In fact, the value of each pole is directly related to the dynamic characteristics of the corresponding vibration mode. Thus, using the root locus method, it is possible to evaluate the modifications imposed on the structure in terms of the natural frequencies and the damping coefficients. The main frequencies and the types of global vibration modes of the tower-DVA system are shown in Fig. 4.

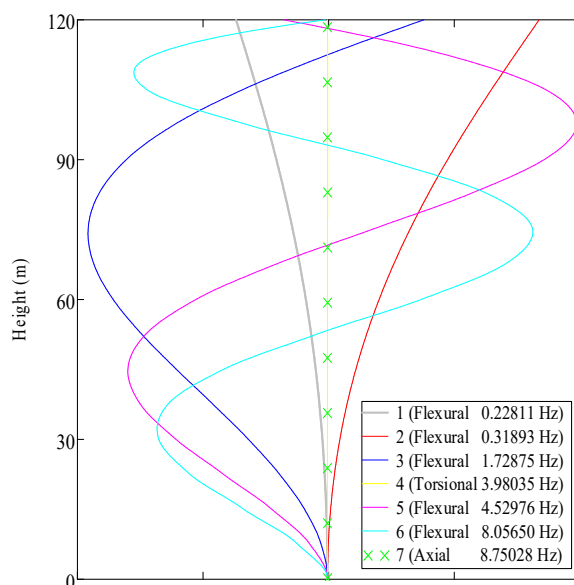


Figure 4. Normalized modes of vibration (displacements transverse to the tower).

The function of the passive vibration absorber is to detune the fundamental frequency of the tower with respect to the proposed excitation frequency, since the fundamental frequency of the tower without vibration absorber, which is equal to 0.29745 Hz, becomes be equal to 0.22810 Hz, for the case of the tower-DVA assembly. In addition, the 2nd vibration frequency (0.31889 Hz) is slightly higher than the fundamental frequency of the tower without absorber. However, such detuning is done by reducing the natural frequency of the structure, i.e., leaving the tower even more flexible. This low flexibility of the tower has been the subject of research that seeks to develop the so-called soft towers, in order to make them more competitive solutions in the market, since, great savings could be reached in case the dogma of great distances between eigenfrequency and exciting frequency is disregarded (Lange and Elberg, 2018 [32]).

#### 4.2 Hybrid vibration control of tower

It is possible to improve the dynamic behavior of the tower (to reduce the intensity and number of vibration cycles) when implementing the hybrid vibration control. Thus, with the passive vibration absorber being designed for the two translational degrees of freedom according to the X and Z directions, the same parameters for the dynamic hybrid vibration absorber are used and the design is complemented with the determination of the optimal control variables to be introduced by the hydraulic actuators.

For the determination of the system state feedback gain matrix  $[KG]$ , Eq. (32), it is necessary to solve the matrix equation of Ricatti, Eq. (33), to obtain the matrix  $[P]$ . For this, the matrices of state ponderation  $[Q]$  and control ponderation  $[R]$  of the system were obtained through an analysis process about: required control (amplitude of displacements and velocities of the controlled tower); energy expended to perform this control (intensity of control forces imposed by the hydraulic actuators); building (dimensions for the vibration absorber and range of stiffness and damping constants found on the market, for springs and viscous dampers); and operability and maintenance (range of displacement amplitudes and velocities of the control device, so as to allow the operation of this within the tower, such as, for example, the limitation of displacement as a function of the space at the top of the tower for electrical and safety equipments and movement of the absorber).

The control ponderation  $[R]$  matrix was taken equal to the identity matrix. The state ponderation  $[Q]$  matrix was initially taken from the order identity matrix and after adjustments made according to

the reasons explained in the previous paragraph:  $Q_{\frac{N}{2}-1, \frac{N}{2}-1} = 10^{12}$  (ponderation element of the top of the tower displacement) and  $Q_{\frac{N}{2}, \frac{N}{2}} = 10^{10}$  (ponderation element of the DVA displacement).

### 4.3 Active vibration control of tower

The procedure for obtaining the gain matrix  $[KG]$  of the system for active control is identical to the hybrid system, and the same  $[Q]$  state and  $[R]$  control ponderation matrices are used. However, in the state matrix  $[A]$  containing the damping and stiffness matrices, the damping and stiffness absorber coefficients are zero, since there are no springs or dampers in the active control system (there are only hydraulic actuators). The mass matrix of the tower-DVA coupled system remains the same.

### 4.4 Parametric analysis of control systems

In order to compare the performances of the passive, hybrid and active control systems, simulations were made of the response of the controlled tower, the output of the vibration absorber and the control forces as a function of the mass ratio ( $\bar{\mu}$ ), which is the mass ratio of the absorber vibration and overall structure.

For plotting the graphs presented, the mass ratio was varied and the other parameters of the absorber, such as stiffness and damping, were recalculated for each mass ratio value, in order to maintain the tuning of the frequency of the absorber with the frequency of the tower, according to Table 3.

Table 3. Parametric analysis of control systems.

Mass ratio $\bar{\mu}$ (%)	Modal mass ratio $\mu$ (%)	Frequency ratio $f$	DVA stiffness $k_t$ (N/m)	DVA damping $c_t$ (kg/s)
1.0	6.217	0.941	2.64153 E4	4.44880 E3
2.0	12.434	0.889	4.71495 E4	1.15540 E4
3.0	18.651	0.843	6.35067 E4	1.95797 E4
4.0	24.869	0.801	7.64536 E4	2.79219 E4
5.0	31.086	0.763	8.67169 E4	3.62791 E4
7.5	46.629	0.682	1.03960 E5	5.63376 E4
10.0	62.171	0.617	1.13317 E5	7.45715 E4
12.5	77.714	0.563	1.17953 E5	9.08481 E4
15.0	93.257	0.517	1.19692 E5	1.05310 E5
17.5	108.800	0.479	1.19625 E5	1.18167 E5
20.0	124.343	0.446	1.18427 E5	1.29632 E5

In the graph shown in Fig. 5a, the modal mass ratio  $\mu$  increases linearly with the mass ratio  $\bar{\mu}$ ; and the ratio  $f$  between the angular frequencies is inversely proportional to the mass ratio  $\mu$ , which is the expression for the required tuning of the absorber under optimum conditions according to Den Hartog's theory. Fig. 5b shows an increasing DVA stiffness up to a maximum value (1.19692 E5 N/m) around the value of 15% of the mass ratio, from which the stiffness decreases slightly. In addition, an almost linear DVA damping behavior is observed as the mass ratio is increased.

In Fig. 6a is shown the graph of the displacement r.m.s. (root mean square) ratio between the values of the tower top controlled and without control, for the three types of control studied (purely passive, hybrid and purely active), as a function of mass ratio  $\bar{\mu}$ . As expected, hybrid, active and passive control systems require, in this order, a smaller amount of DVA-mass to achieve the same level of control. For example, at a mass ratio of 0.03, the passive system reduces the displacement

r.m.s. from the top of the controlled tower to a value that is equivalent to 6.1% of the uncontrolled tower top displacement r.m.s.; while the hybrid and active systems reduce the displacement r.m.s of the top of the controlled tower to 3.7% and 4.7% of the displacement r.m.s. of the tower top without control, respectively.

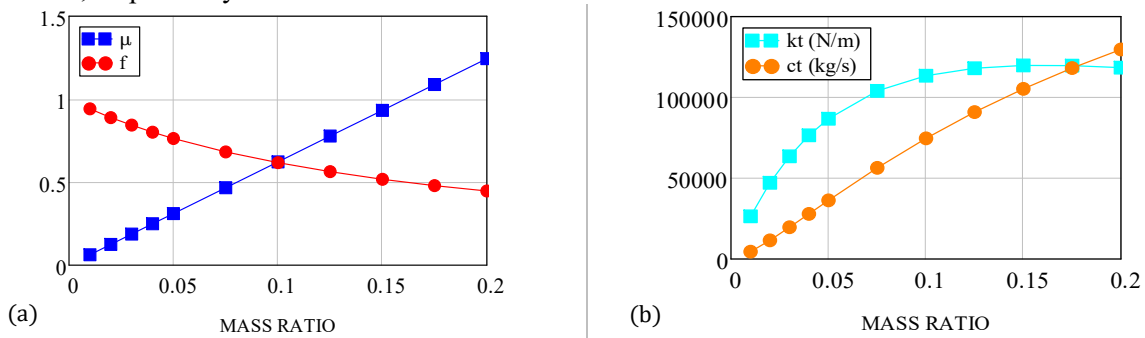


Figure 5. Graphs of: (a)  $\mu$  and  $f$  versus  $\bar{\mu}$ ; (b)  $k_t$  and  $c_t$  versus  $\bar{\mu}$ .

Additionally, it can be observed that the passive control system presents better performance for a mass ratio around 7.5%, which loses efficiency for higher mass ratios. However, the efficiency in the control of displacements of the tower top, for the hybrid and active systems, increases with the growth of the mass ratio until it reaches a horizontal asymptotic behavior from a mass ratio around 10%. Nonetheless, for values of mass ratio with this value or higher, the feasibility of using the vibration absorber is hampered, if not impossible.

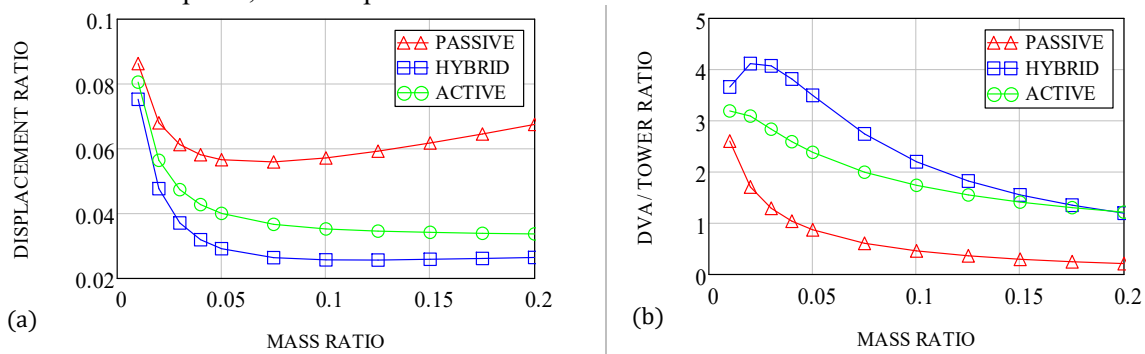


Figure 6. Displacement r.m.s. ratio: (a) tower top controlled and without control; (b) DVA and tower top controlled.

Another important aspect in this parametric analysis, which is comparative among the proposed control systems, refers to the energy required to achieve a certain level of control. It is possible to observe that the hybrid and active systems have similar behavior, both with respect to the tower response (Fig. 6a) and with respect to the vibration absorber response (Fig. 6b). In Fig. 6a, the control behavior of the hybrid system is better than that of the active system because, on average, the r.m.s. displacement of the tower top is 24.3% lower when the hybrid control is used. In addition, Fig. 6b shows that, on average, the ratio between displacement r.m.s. of the absorber and tower top controlled in the hybrid system is 26.7% higher than that of the active system.

Finally, comparing the data of the graph of Fig. 7, it is observed that the hybrid system requires a control force of a smaller magnitude in relation to a purely active system, because the curves have practically the same behavior, being only separated vertically, on average, by a value of  $1.846 \text{ E}4 \text{ N}$ . The previous comments establish and confirm some advantages of the hybrid control system in relation to the purely active system.

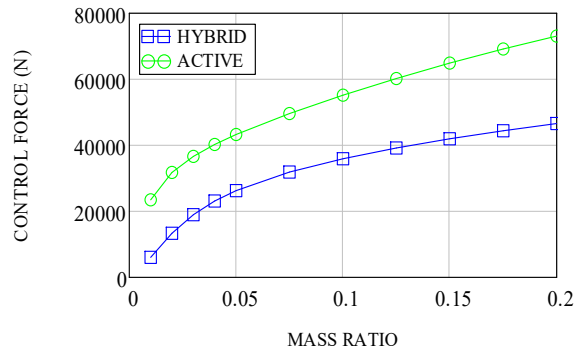


Figure 7. Control force r.m.s. applied to the top of the tower.

#### 4.5 Transient responses

The harmonic excitation to which the tower is subjected was applied for a time of only 5 s, from which the excitation ceases and the tower-DVA assembly vibrates freely (Fig. 8 and Fig. 9). This excitation simulates an intensity of a tipic wind gust. Table 4 shows the tower top maximum and r.m.s. displacements of uncontrolled and controlled systems; as well as the percentage reduction of such displacements.

Table 4: Tower top displacement due to transient excitation.

Without control		Passive control		Hybrid control		Active control	
Maximum (m)	r.m.s. (m)	Maximum (m)	r.m.s. (m)	Maximum (m)	r.m.s. (m)	Maximum (m)	r.m.s. (m)
0.56497	0.23126	0.23190	0.07451	0.15757	0.05463	0.19671	0.06559
Percentage reduction of r.m.s. (%)							
Without control → Passive control		Passive control → Hybrid control		Without control → Active control			
67.78		26.68		71.64			

Figure 8 shows the graph of uncontrolled and passively controlled top of tower displacements, from which we can observe a high reduction of such displacement values; as shown in Table 4. There is a reduction of 67.78 and 71.64% in the r.m.s. of the tower top displacement in relation to the uncontrolled case with the introduction of the passive and active DVA, respectively, in the tower structural system.

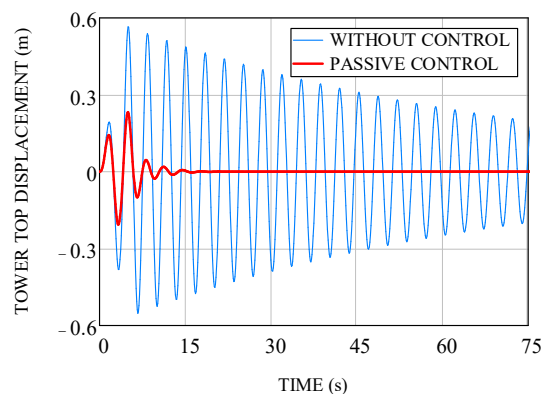


Figure 8. Tower top displacement without control and under passive control (transient excitation).

For comparisons of passively and hybridly controlled tower top displacements, the graphs of Fig. 9a were plotted. It is observed that the hybrid system performs better than the purely passive system, reducing the r.m.s. of the tower top displacements by 26.68% in relation to the displacement of the top of the passively controlled tower. In addition, it is noticed that the vibration stops earlier

(Fig. 9a) and that the vibration peak is smaller (Table 4) when using the hybrid control system.

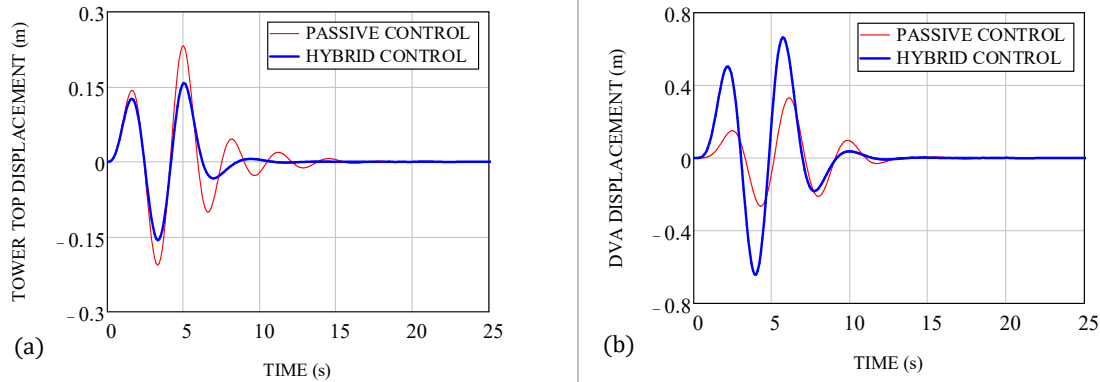


Figure 9. Displacements of the: (a) tower top and (b) DVA under passive and hybrid control (transient excitation).

It is shown in Fig. 9b the graph of the displacements of the vibration absorber for tower equipped with passive and hybrid control. It should be noted that the absorber response becomes more rapid with the introduction of the actuators from the hybrid and active control systems, making these systems more suitable for situations where rapid control action is required for efficiency and robustness of the control system (as in the case of control of seismically excited structures).

Finally, the graph of the control force acting on the dynamic vibration absorber with reaction at the top of the tower is shown in Fig. 10. By means of the values of the control forces, one has an idea of the energy required for the control of the tower by the hybrid system. It is important to note that there is a lag (about 1.3 s) between the peaks of the control force graphs (Fig. 10) and the vibration absorber displacement (Fig. 9b), so that the peak of the control force excites the vibration absorber, and it subsequently moves toward its displacement peak to control the structure of the tower.

#### 4.6 Steady-state responses

In this section, the structure of the tower-DVA submitted to stationary resonant harmonic excitation is analyzed, for which an analysis time of 100 s is used to calculate the r.m.s. values. Table 5 shows the tower top maximum and r.m.s. displacements of uncontrolled, passive and active controlled system.

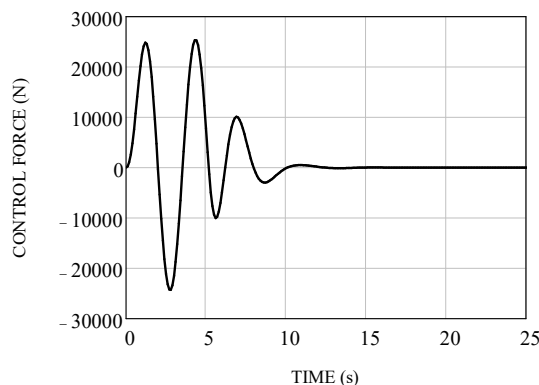


Figure 10. Control force applied by hydraulic actuators (transient excitation).

In Fig. 11 is shown the graph of the uncontrolled and passively controlled top of the tower, from which we can observe the high efficiency of the passive system in the control of the two 1st vibration modes (XY and YZ) of the tower, in view that the vibration absorber has been tuned to such frequencies. According to the data of Table 5, with the use of the passive and active systems, it is observed that there is a reduction of 93.87 and 95.26% in the r.m.s. of the tower top displacement in relation to the case without control, respectively.

Table 5. Tower top displacement due to permanent excitation.

Without control		Passive control		Hybrid control		Active control	
Maximum (m)	r.m.s. (m)	Maximum (m)	r.m.s. (m)	Maximum (m)	r.m.s. (m)	Maximum (m)	r.m.s. (m)
6.02837	2.91768	0.25723	0.17884	0.15757	0.10828	0.19768	0.13833
Percentage reduction of r.m.s. (%)							
Without control → Passive control		Passive control → Hybrid control		Without control → Active control			
93.87		39.46		95.26			

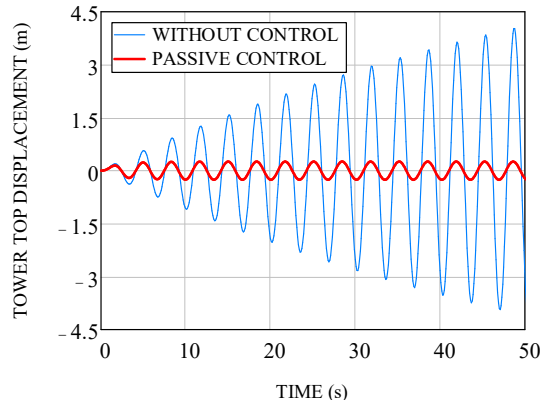


Figure 11. Tower top displacement without control and under passive control (stationary excitation).

For the comparison of the passive and hybrid control systems, the graph of passively controlled and hybridly controlled tower displacements (Fig. 12a) and Table 5 data are analyzed; in which it is possible to improve the performance of the control system, since the r.m.s. value of tower top displacements is reduced in 39.46% compared to the tower top displacements controlled passively.

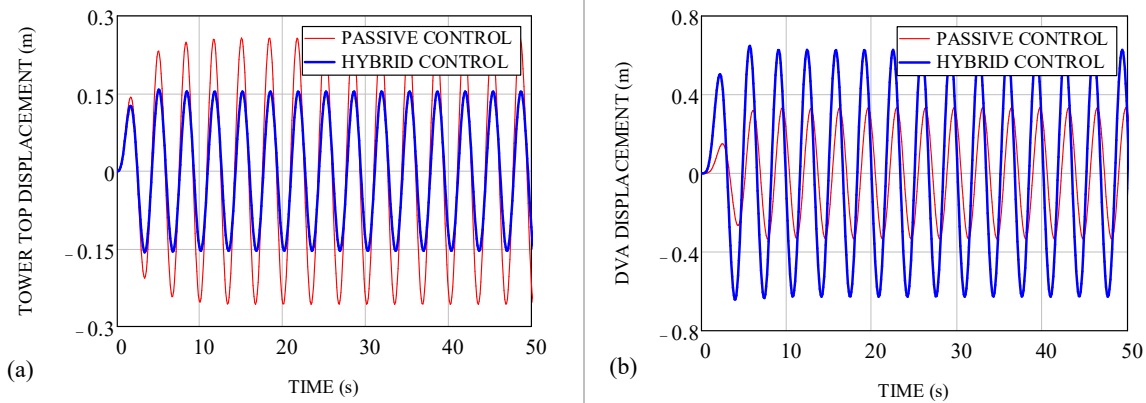


Figure 12. Displacements of the: (a) tower top and (b) DVA under passive and hybrid control (stationary excitation).

In this way, the introduction of active control improves the robustness of the system in situations that require to refine/improve the vibration control. On the other hand, the passive control considerably reduces the displacements, so that the control system works well in situations of loss of electric power and, consequently, impossibility of actuation of the active system. However, when the structure is subjected to a detuned excitation in relation to the prevailing vibration frequency of the tower, the active control actuators begin to correct or improve/refine the behavior of the purely passive control, since the active control also works well for a frequency of excitation not tuned at any of the modal frequencies of the uncontrolled tower structure. Such performance of hybrid and active systems may become, in certain cases of practical application, indispensable for the proper functioning and safety of the tower structure and its users.

Corroborating with the above findings, in Fig. 12b is shown the graph of the displacements of the vibration absorber for tower equipped with passive and hybrid control, in which the most effective action of the hybrid control is observed, since the dynamic vibration absorber responds more rapidly and significantly to the action imposed on the structure of the tower-DVA assembly. Finally, in Fig. 13 is shown the graph of the control force exerted by the actuators that act on the dynamic vibration absorber and have a reaction at the top of the tower.

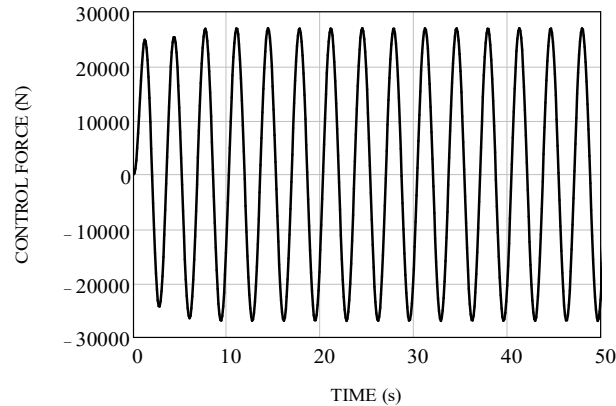


Figure 13. Control force applied by hydraulic actuators (stationary excitation).

The values of the control forces provide a perception of the energy required for the control of the tower by the hybrid system. In addition, the maximum control force (between 20.0 and 30.0 kN) is perfectly possible to be applied using an electronically controlled hydraulic pump with a working pressure between 1000 and 1500 bar, coupled to a piston with a cross-sectional area of 200 cm<sup>2</sup> that highlights the technical feasibility of the proposed control system.

## 5 Conclusions

After analysis developed in this paper, it is observed that the vibration absorbers proposed, both passive and hybrid, presented efficiency in the tower control vibration when the tower-absorber assembly is submitted to a harmonic action resonant to the 1st tower mode of vibration.

The results of the modal analysis performed for both the beam and shell finite element model are similar, especially in relation to the 1st vibration mode of the tower. Therefore, the model represented by beam FE can be used as representative of the tower dynamic behavior when it is submitted to the resonant excitations to its fundamental frequency. With this, the action of the floating part of the wind was modeled by resonant harmonic forces, considering the tendency that there is the excitation of the fundamental way of the tower. Since the increasing intensity of the wind forces with height relative to ground level, the increase of the horizontal displacements to the tower with respect to the height in the 1st mode of vibration and the mass concentrated in the top (nacelle), of the same order of magnitude of the tower mass, are factors that contribute to excitation of the 1st mode of vibration of the tower.

Three types of absorbers were then comparatively studied: tuned mass damper (TMD), active mass damper (AMD) and hybrid mass damper (HMD). The HMD, the main contribution of this paper, reached excellent levels of vibration reduction for the tower subjected to harmonic actions, in a transient and permanent (stationary) regime, resonating with the first vibration mode of the structure without absorber.

In view of the obtained results, it is verified that the purely passive system is quite efficient in the control of vibrations of the excited tower according to the 1st vibration mode for which the absorber is tuned. Hybrid and active systems have been able to significantly improve passive system performance. It can be noted that the absorber response becomes faster with the introduction of hydraulic actuators of the hybrid control system, making this system suitable for situations where rapid control action is required for effectiveness and robustness of the system.

It is concluded, therefore, that the results of this work involve contributions of immediate

practical interest, since the research develops subsidies for structural analysis and vibration control of the towers for multi-megawatt wind turbines to be implanted in Brazil considering the recent growth of the country's wind potential.

## References

- [1] Hau, E. (2006). Wind turbines: fundamentals, technologies, application, economics. 2nd. Edition, Springer, Munich.
- [2] GWEC (2019). Global Wind Energy Council. Global statistics. Brussels. Available at: <http://gwec.net/global-figures/graphs/>.
- [3] Abecólica (2018). Energia eólica ultrapassa marca de 14 GW de capacidade instalada. Notícias, Agência ABEEólica. Available at: <http://abeeolica.org.br/>.
- [4] Burton, T., Jenkins, N., Sharpe, D., Bossanyi, E. (2011). Wind energy handbook. 2nd Edition, John Wiley & Sons, Chichester.
- [5] Manwell, J. F., McGowan, J. G., Rogers, A. L. (2009). Wind energy explained: theory, design and application. 2nd Edition, John Wiley & Sons, Chichester.
- [6] Juárez, A. A., Araújo, A. M., Rohatgi, J. S., Oliveira Filho, O. D. Q., (2014). Development of the wind power in Brazil: political, social and technical issues. *Renewable and Sustainable Energy Reviews* 39: 828–834.
- [7] Atlas..., (2017). Atlas eólico e solar de Pernambuco. Available at: <http://www.atlaseolicosolar.pe.gov.br/>
- [8] Yoshida, P. E., (2006). Wind Turbine Tower Optimization Method Using Genetic Algorithm. *Wind Engineering* 30(6): 453-470.
- [9] Menezes, E. J. N.; Araújo, A. M.; Rohatgi, J. S.; Foyo, P. M. G., (2018). Active load control of large wind turbines using state-space methods and disturbance accommodating control. *Energy* 150: 310-319.
- [10] evinsDen Hartog, J. P. (1947). Mechanical vibrations. 3rd edition, McGraw-Hill, New York.
- [11] Associação Brasileira de Normas Técnicas (ABNT), NBR 6123: 1988, Forças devidas ao vento em edificações, Rio de Janeiro, 1988.
- [12] Blevins, R. D. (2001). Flow-induced vibration, 2nd Edition, Krieger Publishing Company, Malabar.
- [13] Rao, S. (2011). Mechanical vibrations. 5nd edition, Prentice Hall, United States of America.
- [14] Moutinho, C. M. R. (2007). Controlo de vibrações em estruturas de engenharia civil. Ph.D. Thesis (in Portuguese), Porto University, Portugal.
- [15] Junkins, J. L. and Kim, Y. (1993). Introduction to dynamics and control of flexible structures. American Institute of Aeronautics and Astronautics, Washington, D.C.
- [16] Clough, R. W. and Penzien, J. (2003). Dynamics of structures. 3rd edition, Computers & Structures, Berkeley.
- [17] Chopra, A. K. (2012). Dynamics of structures: theory and applications to earthquake engineering. 4nd Edition, Practice Hall.
- [18] Humar, J. L. (2002). Dynamics of Structures. 2nd edition, A.A. Balkema Publishers, Ottawa.
- [19] Meirovitch, L. (1990). Dynamics and control of structures. JohnWiley & Sons, New York.
- [20] Ogata, K. (1997). Modern control engineering. 3rd edition, Prentice Hall, United States of America.
- [21] Lyapunov, A. M., (1992). The general problem of the stability of motion. *International Journal of Control* 55 (2): 531-773.
- [22] Kwakernaak, H. and Sivan, R. (1972). Linear optimal control systems. Wiley & Sons, New York.
- [23] Lima, D.M.; López-Yáñez, P. A.; Silva, J. W., (2018). Análise da estabilidade elástica em torres tubulares de aço para aerogeradores de eixo horizontal. *Revista da Estrutura de Aço* 7 (2): 100-119.
- [24] Siemens (2014). Siemens D3 platform – 3.0-MW and 3.2 – MW direct drive wind turbines: Reduced complexity, increased profitability. Erlangen, Germany. Available at: [https://www.energy.siemens.com/br/pool/hq/power-generation/renewable/wind-power/platform20brochures/D3%20Onshore%20brochure\\_ENGLISH\\_Apr2014\\_WEB.pdf](https://www.energy.siemens.com/br/pool/hq/power-generation/renewable/wind-power/platform20brochures/D3%20Onshore%20brochure_ENGLISH_Apr2014_WEB.pdf).

- [25] Cook, R. D., Malkus, D. S., Plesha, M. E., Witt, R. J. (2002). Concepts and applications of finite element analysis. 4nd edition, John Wiley & Sons, Madison.
- [26] Mathcad 15.0 M020 (2012). PTC software.
- [27] ANSYS release 14.5 (2012). Swanson Analysis Systems Inc.
- [28] Lima, D. M. (2018). Análise da estabilidade elástica, análise dinâmica e controle de vibração em torres tubulares de aço para aerogeradores de eixo horizontal. Ph.D. Thesis (in Portuguese), Federal University of Pernambuco, Brazil.
- [29] Asibor, A. I., Garcia, J. R., Ramos, M. C., Silva, E. C. M., Araújo, A. M., (2015). Wind turbine performance and loading calculations using aeroelastic modelling. In: 23 th International Congress of Mechanical Engineering, ABCM, Rio de Janeiro.
- [30] Franco, M. (1993). Direct Along-wind Dynamic Analysis of Tall Structures. Boletim Técnico da
- [31] Housner, G. W., Bergman, L. A., Caughey, T. K., Chassiakos, A. G., Claus, R. O., Masri, S. F., Skelton, R. E., Soong, T. T., Spencer, B. F., Yao, J. T. P., (1997). Structural control: past, present and future. Journal of Engineering Mechanics 123 (9): 897-971.
- [32] Lange, H. and Elberg, C., (2018). Development of soft towers for wind turbines. In: Wind Turbine Towers, Bremen.